prosthesis

MDPI

Article

The Influence of Various Superstructure Materials on Stress Distribution for Implant-Supported Prosthesis: Three-Dimensional Finite Element Analysis

Rawan Mufeed Jameel * and Aseel Mohammed Al-Khafaji

Department of Prosthodontics, College of Dentistry, University of Baghdad, Baghdad 10071, Iraq; aseel.khafaji@codental.uobaghdad.edu.iq

* Correspondence: roseroro942@gmail.com; Tel.: +96-47905135277

Abstract: In different applied load scenarios, this study evaluates the distribution of stress in the implant and bone exerted by zirconia, lithium disilicate, and cobalt chromium alloy. A 3D virtual model of a mandibular three-unit implant-supported prosthesis was created using SolidWorks 2022. The model featured two 12-mm Straumann Ti-Zr (Roxolid) implants with diameters of 4.5 mm and 4 mm. Zirconia, lithium disilicate, and cobalt chromium alloy were used as superstructure materials. Vertical loads of 100 N and 200 N were applied to the central fossa of the implant-supported prosthesis. The finite element analysis demonstrated that doubling the applied load leads to a proportional increase in von Mises stress on both the implant and bone in a mandibular posterior three-unit implant-supported prosthesis model. Zirconia and chromium cobalt as superstructure materials result in similar stress levels due to their closely matched elastic moduli of 200 GPa and 218 GPa, respectively. In contrast, lithium disilicate leads to the highest stress levels, which is attributed to its lower elastic modulus of 95 GPa. These findings highlight the critical role of superstructure material properties in stress distribution. Zirconia emerges as the preferred material for implant-supported prosthetics due to its favorable stress distribution.

Keywords: superstructure materials; implant-supported prosthesis; dentistry; finite element analysis; stress distribution

check for updates

Citation: Jameel, R.M.; Al-Khafaji, A.M. The Influence of Various Superstructure Materials on Stress Distribution for Implant-Supported Prosthesis: Three-Dimensional Finite Element Analysis. *Prosthesis* **2024**, *6*, 1133–1148. https://doi.org/10.3390/prosthesis6050082

Academic Editors: Roberto Sorrentino, Fernando Zarone and Gennaro Ruggiero

Received: 31 July 2024
Revised: 9 September 2024
Accepted: 11 September 2024
Published: 19 September 2024

Copyright: © 2024 by the authors. Licensee MDPI, Basel, Switzerland. This article is an open access article distributed under the terms and conditions of the Creative Commons Attribution (CC BY) license (https://creativecommons.org/licenses/by/4.0/).

1. Introduction

In the last decades, dental implants have helped millions of patients live better lives and have demonstrated a high success rate [1]. Dental implantation has become a standard procedure with high success rates, relying on achieving osseointegration between the implant surface and surrounding bone tissue [2]. Achieving the ideal implant properties—such as their biomechanical and surface characteristics—can increase the clinical success of dental implants [3].

Usually, dental implants are positioned inside the jaw's cortical bone to support and stabilize prosthetic restorations [4]. Dental implants can be made of various materials, and amongst them, titanium and titanium alloy were the materials of choice for dental implants for many years because of their biocompatibility [5]. Ti-Zr alloys are highly biocompatible materials and demonstrate superior mechanical properties and better bone implant contact in the initial healing phase than commercially pure titanium [6]. Recently, there have been zirconia fittings that promise to be more aesthetically pleasing, giving titanium dental implants more competition [7].

In light of the demands of minimally invasive dentistry, the introduction of a new generation of particle-filled and high-strength ceramics, hybrid composites, and technopolymers in the last ten years has provided an extensive palette of dental materials, expanding the clinical indications in fixed prosthodontics. Furthermore, patients' demand for non-metallic materials has dramatically increased in the past several years, often as a result of

metal anxiety or purported allergies. Therefore, in an effort to shed light on the characteristics, indications, and limitations of the new players in the prosthetic scene, scientific studies have been progressively focusing on such materials, especially zirconia and lithium disilicate [8]. Implant-supported prostheses can be made with a variety of prosthetic materials. Although it is widely agreed that the prosthetic material has no effect on implant longevity, the selection of this material remains contentious. Implant stability is considered one of the most important factors affecting healing and successful osseointegration of dental implants [9].

According to Skalak et al., loading an implant composed of metal or porcelain, or another hard occlusal material, may cause high-intensity loading between the implant and the supporting bone. While it has stress-absorbing qualities, a material with a low modulus of elasticity can shield the surrounding bone from potential damage due to the size of the load [10]. Alloys containing cobalt and chromium (Co–Cr) are utilized in dental prosthetics for crowns, implants, bridges, and removable partial denture restorations. For prolonged usage, they have the required biocompatibility and performance because of their mechanical qualities, which include high strength, hardness, and resistance to tarnish and corrosion [11]. The long-term effectiveness of an implant therapy is thought to be significantly influenced by the occlusal loading of osseointegrated implants. Few studies have examined provisional restoration materials for implant-supported fixed prostheses, despite the fact that several have examined the evaluation of stress distribution by definitive restoration materials [12].

Ceramic composites made of alumina and zirconia have become increasingly popular in dentistry and orthopedic joint replacements in the twenty-first century [13]. Zirconia is a high-strength ceramic material that increases the potential applications and design for dental implants and all-ceramic restorations [14]. Many factors that impact the mechanics of toughening and, consequently, the mechanical characteristics must be taken into account when designing high-performance zirconia composites. These factors include the kind and quantity of the stabilizer as well as the sintering procedure [15]. The choice of material utilized on the occlusal surface of prostheses supported by implants is crucial because certain materials have the potential to transfer damaging stresses to the contact between the implant and the alveolar bone. For implant-supported prostheses, many prosthetic materials are recommended. The selection of the prosthetic material is a contentious matter; however, most people agree that the prosthetic material has no bearing on implant longevity [16].

It is feasible to simulate a state with 3D-FEA that is not achievable in a clinical investigation. As a result, conventional finite elements have emerged as a helpful method for researching implant dentistry stress distribution [17]. Appropriate planning of the materials used for the implant prosthesis's substructure and superstructure is crucial for ensuring long-term clinical success. The transmission of functional loads and stress distribution in a bone-implant-prosthesis assembly are significantly influenced by the material qualities and spatial geometric configuration model of each component [18]. These elements cooperate with one another in the oral environment; thus, the arrangement of the ingredients is crucial. It is advised to minimize these stressors because the type and extent of the intraoral strains are unknown. Therefore, many doctors are interested in discovering appropriate dental materials that address biomechanical limitations and maximize function and aesthetics [19].

Prostheses with zirconia substructures can have a significant frequency of minor mechanical problems despite generally having a very good survival rate [20]. Clinicians can now obtain excellent aesthetic outcomes with dental prostheses because of modern materials and processes that standardize and yield accurate, reproducible results, particularly when it comes to a product's long-term durability and functionality [21].

One of the best computational tools for determining the stress on implant-supported restorations is probably the finite element method (FEM) [22]. The finite element method has several advantages over other methods for evaluating stress around dental implant systems, such as the accurate representation of complex geometries, ease of model modi-

fication, and representation of the internal state of stress [23]. When a zirconia abutment was used, the implant's von Mises stress values decreased while those of the abutment increased [24].

Cobalt–chromium (Co–Cr) alloys are categorized as primarily base-metal alloys and are well-known for their orthopedic and dental biomedical uses [25]. Lithium disilicate ceramic monolithic occlusal onlays are a dependable treatment choice for full-mouth rehabilitations in patients with significant tooth wear, according to data analysis spanning up to 11 years [26]. Recent years have witnessed a sharp rise in the demand from patients for non-metallic materials, often due to purported allergies or metal phobia. To shed light on the characteristics, uses, and limitations of the new players on the prosthetic scene, scientific study has consequently been gradually concentrating on these materials, especially lithium disilicate and zirconia [8].

It has been demonstrated that fully anatomical e.max CAD crowns grown in vitro have fracture resistance appropriate for posterior monolithic restorations [27]. The superior soft tissue response quality of LS_2 is one of its strongest qualities. This material demonstrates excellent biocompatibility in vitro, as evidenced by its minimal plaque retention as well as its ability to adhere to and multiply human epithelial cells [28]. Analyzing the levels of inflammation indicators in the gingival crevicular fluid in vivo revealed that no inflammatory reactions were observed in the presence of LS_2 restorations; zirconia restorations yielded similar results [29]. Apart from its superior mechanical qualities and exceptional biocompatibility, lithium disilicate also has very good aesthetic qualities, particularly in terms of translucency, which is almost 30% higher than that of traditional zirconia [30]. Zirconia has good radiopacity, excellent biocompatibility, and reduced plaque retention compared to titanium in both vitro and in vivo settings. It is also water insoluble and has very little sensitivity to corrosion in the oral environment [31]. Since zirconia lacks the translucency of glassy ceramics, it is typically regarded as an opaque restorative material with less appealing optical and aesthetic qualities [32]. Finite element analysis (FEA) in three dimensions (3D) is a useful technique for forecasting how a material's stress distribution will change under external strain. The majority of dental structures are dynamically impacted by occlusal force, and finite element analysis (FEA) has previously shown itself to be an effective tool for determining how implants and restorative materials distribute stress [33].

This study aimed to assesses the peri-implant stress exerted by various materials (such as zirconia, lithium disilicate, and cobalt chromium alloy) under various applied load scenarios, applying finite element analysis to examine how various occlusal materials affect the distribution of stress in implants and bone.

The null hypothesis was that the modulus of elasticity of superstructure materials from different materials does not have an effect on the distribution of stresses in implants and bone [34]. It is critical to comprehend how chewing loads are transmitted from the implant prosthetic components to the surrounding bone tissue in order to guarantee the long-term viability of a dental implant. The load type, the interface between the bone and the implant, the fixture's shape and materials, the quantity and quality of the bone, and other factors all affect how the stress is distributed [35].

2. Materials and Methods

A three-dimensional virtual model of a mandibular posterior three-unit implant-supported prosthesis was created using the following equipment:

1. Personal computer GPU: NVIDIA GEFORCE RTX 3080 10GB, Ram:64GB, CPU: Core I9 10900K, Power Supply: 850W, Motherboard:Z490 AORUS ELITE AC.
2. For modeling, rendering and simulation the implant-supported prosthesis—BLENDER 4.0 program.
3. ANSYS finite element program for stress analysis (ANSYS Version 2020 R1).
4. For modeling the implant and bone—SolidWorks 2022.
5. Screw-shaped dental implant system—The Straumann® BLX Implant, Figure 1.



(**a**) (**b**)

Figure 1. Implant fixture (Straumann® BLX Implant) designed by SolidWorks 2021: (**a**) 4.5 mm in diameter; (**b**) 4 mm in diameter.

To generate finite element (FE) models, a three-dimensional geometry of a mandibular posterior three-unit implant-supported prosthesis was used as the starting point using the CAD design software SolidWorks 2022.

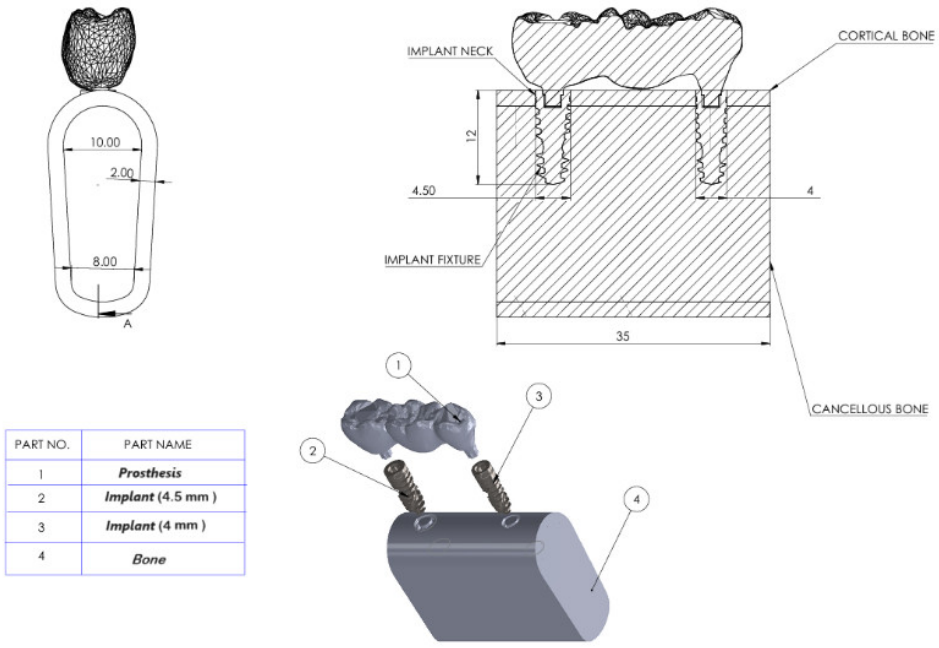
A mandibular posterior bone block was constructed, and the implants were inserted into the block, the mandibular bone was modeled as an 8-mm thick cancellous core encircled by 2-mm thick cortical bone. The bone height was 25 mm, which is in line with previous studies [36–38].

In this study, type 2 bone quality was employed. Starting from the second premolar region and ending at the retromolar pad area, the model represents a three-dimensional segment of the mandibular bone, Figure 2.

The dimensions of the three-unit implant-supported prosthesis were almost exactly modeled by the dimensions corresponding to natural teeth [39]. The dimensions are presented in Table 1.

Table 1. The dimensions of the mandibular posterior three-unit implant-supported prosthesis.

Area	Dimensions, mm		
	Second Premolar	**First Molar**	**Second Molar**
Buccolingual diameter of crown	8	10.5	10
Buccolingual diameter of crown at cervix	7	9	9
Mesiodistal diameter of crown	7	11	10.5
Mesiodistal diameter of crown at cervix	5	9	8
Cervico-occlusal length of crown	8	7.5	7



PART NO.	PART NAME
1	***Prosthesis***
2	***Implant*** **(4.5 mm)**
3	***Implant*** **(4 mm)**
4	***Bone***

Figure 2. Mandibular posterior three-unit implant-supported prosthesis assembly.

The two Straumann implants employed in this 3D finite element analysis study had a length of 12 mm and a diameter of 4.5 mm in the second molar area and 4 mm in the second premolar area. They were manufactured by Roxolid®, Institute Straumann AG, Basel, Switzerland. The model was drawn, modeled using (SOLIDWORKS 2022) then the x, y, and z coordinates of each node were transferred to the finite element software (ANSYS Version 2020 R1) for analyzing and the processing method, Figure 3.

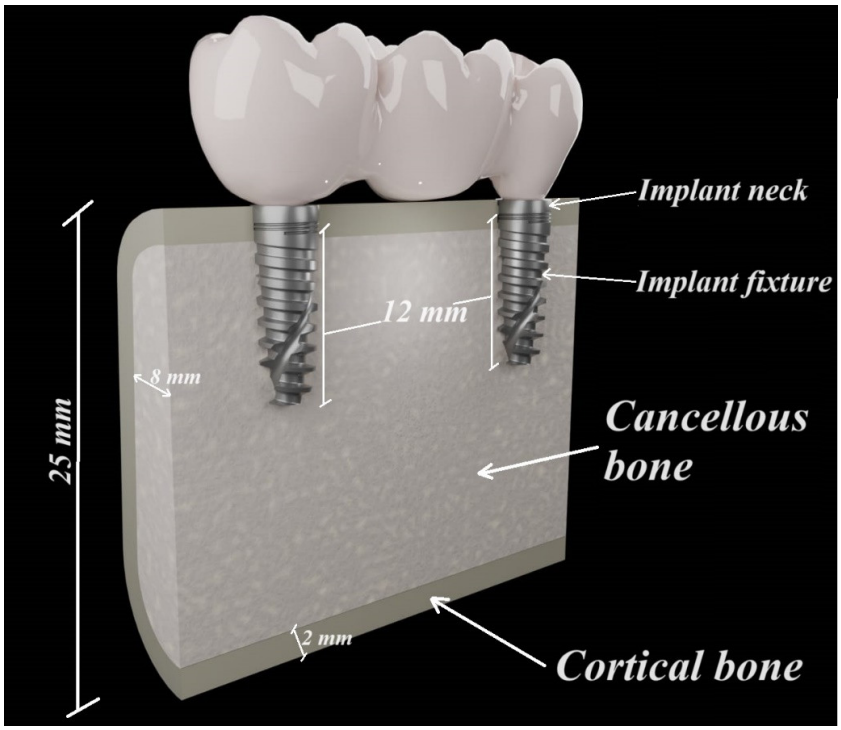


Figure 3. Sectional view of the mandibular posterior three-unit implant-supported prosthesis illustrating the model terminology and dimensions.

In order to stimulate the optimal osseointegration, the implants were securely fixed across their interface in the bone model. This ensured that the implant was completely osseointegrated with the surrounding bone, preventing any movement or sliding at the interface between the implant and the bone. The lower region of the cortical bone was assumed to be fixed in the axial and horizontal direction to avoid the whole model from sinking when applying load to the implant. Depending on the superstructure materials, three distinct models were developed.

In this study, three different prosthetic materials were used for fixed dental prostheses (FDP). These materials are zirconia, lithium disilicate, and cobalt chromium alloy. For dental implants, Ti–Zr implants (Roxolid) were used. All the materials used were assumed to be linearly elastic, homogeneous, and isotropic. The mechanical properties were data supplied by the manufacturers and are shown in Table 2. The deformation or strain of the structure is proportional to the applied force.

Table 2. Mechanical properties of the materials.

Material	Young's Modulus, GPa	Poisson's Ratio
Cortical bone [40]	13.7	0.30
Cancellous bone [40]	1.37	0.30
Ti-Zr implant (Roxolid) [40,41]	100	0.30
Lithium disilicate [42]	95	0.30
Cobalt chromium alloy [40]	218	0.30
Zirconia [43]	200	0.31

The designed model was meshed using tetrahedral elements. A finer mesh was generated at the material interfaces to ensure accuracy of the force transfer, as shown in Figure 4.

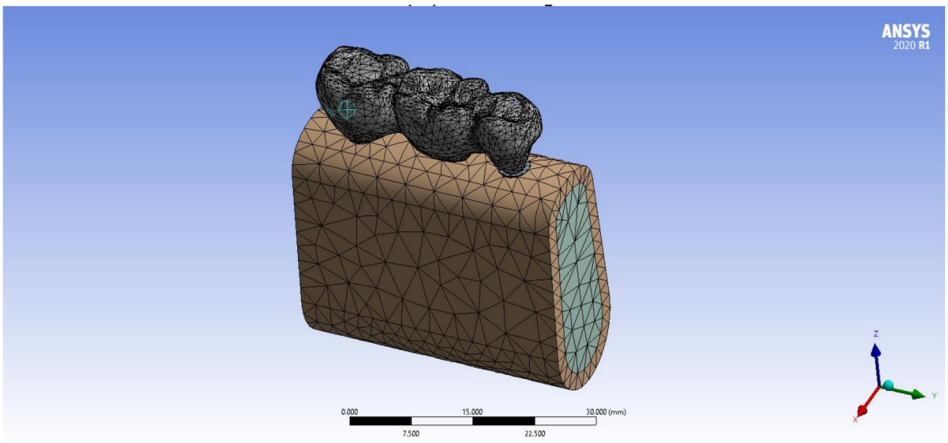


Figure 4. 3D model illustrating the finite element mesh.

The number of elements generated by the mandibular posterior three-unit implant-supported prosthesis model was 54,896 and the number of nodes generated by this model was 95,287.

Axial loading, which occurs when a load is applied on the tooth's long axis, is a desirable force because it distributes the force uniformly across the implant bone surface, as shown in Figure 5. The loads used in this study were 100 and 200 N [44,45]

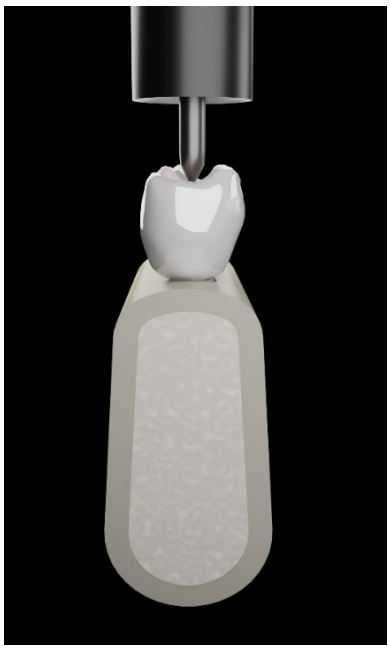


Figure 5. Direction and position of applied loads in the central fossa.

The analysis for each loading condition was performed by means of the Ansys software program (ANSYS Version 2020 R1), which was run on a personal computer with GPU:NVIDIA GEFORCE RTX 3080 10GB, RAM:64GB, CPU:CORE I9 10900K, POWER SUPPLY: 850W, MOTHERBOARD:Z490 AORUS ELITE AC, and the distribution of equivalent von Mises stress was investigated. The calculation time was 30 min for each model being analyzed.

Specified nodes were selected on both sides of the cortical bone, cortical–cancellous bone interface, implant/neck, and implant/apex. These points were fixed for all the models to monitor the stress changes in these models in order to provide a way to select the best design for implant-supported prostheses. Four points were selected at the upper border of the cortical bone and another four points were selected at the cortical–cancellous bone interface. On the cortical bone–implant neck interface, four points were selected in the right and left sides of the second implant-supported premolar and the second implant-supported molar for all of the analyzed models. Seven points at the implant apex–bone interface were selected for the second implant-supported premolar and the second implant-supported molar for all of the analyzed models.

At the middle third of the implants for the implant-supported premolars and implant-supported molars, three points were selected: on the upper junction of the thread to the implant; on the thread tip; and lastly on the lower junction of the thread to the implant.

The experimental data were gathered in principal stress (MPa), which represented the largest load in unit area on the simulated models, as shown in Figure 6.

Analysis of variance (ANOVA) was used for the statistical analysis, the measurement data conforming to the normal distribution were expressed as mean ± standard deviation (±SD), and the comparison between groups was conducted by a one-way analysis of variance. Levene's statistic test was used for the comparison between groups. One-way ANOVA was used to compare the means of all the groups to determine whether there was a statistically significant difference between the groups or not. Levene's test was performed to verify the homogeneity of variance between the groups. A p-value > 0.05 was considered statistically non-significant (NS) and a p-value $\leq$ 0.05 was considered significant (S).

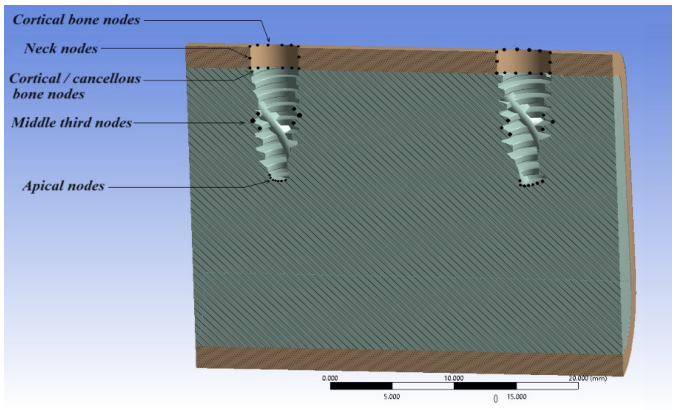


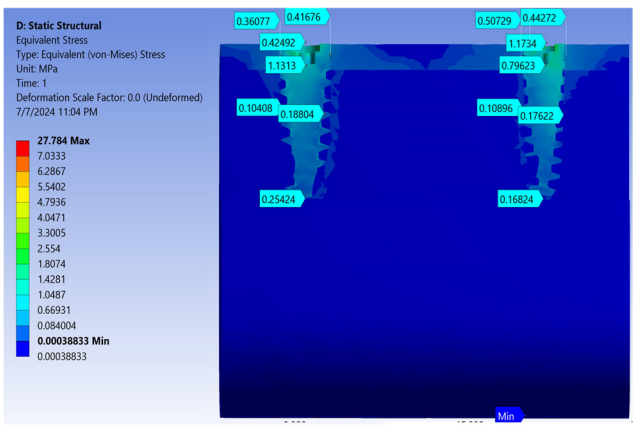
Figure 6. Three-dimensional model illustrating the stress monitoring points.

3. Results

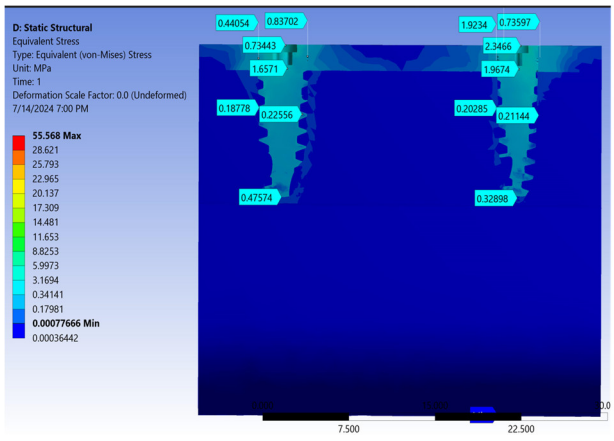
According to the von Mises hypothesis, failure happens when the material's yield strength and the equivalent stress for the real situation are equal. For every node, the von Mises criteria were used to quantify the stress level. This stress analysis, or equivalent stress, is useful for understanding FEA research. This hypothesis states that elastic failure happens when the stressed material's shear strain energy per unit volume equals the shear strain energy per unit volume at the elastic limit point. Most ductile materials are thought to comply with this notion when subjected to different kinds of loading.

The equivalent stress, which calculates the entire state of stress at a preset position based on the Maxwell Huber–Hencky–von Mises hypothesis, reveals the model's local sensitivity to the load under consideration based on its magnitude [46].

Stresses were found at each node in a model by FEA. Results are typically shown as stress contours overlaid on the original model because it is laborious to provide all of the data. The results were represented by the equivalent von Mises stress at selected nodes (37,45), as shown in Figure 7.



(**a**)



(**b**)

Figure 7. *Cont.*

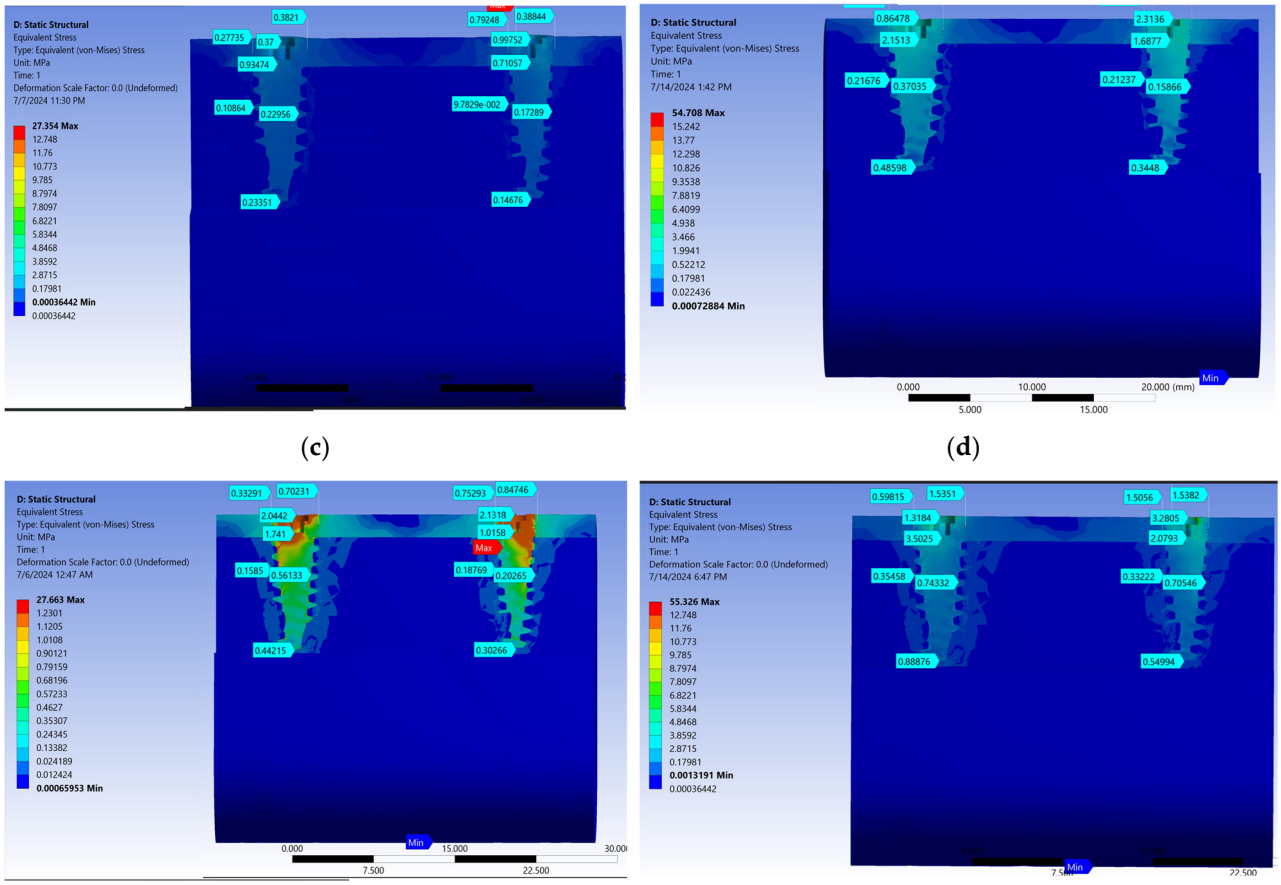


Figure 7. Von Mises stresses of implant-supported model at central fossa with superstructure different materials: (**a**) Zirconia with 100 N applied load; (**b**) Zirconia with 200 N applied load; (**c**) Cobalt chromium alloy with 100 N applied load; (**d**) Cobalt chromium alloy with 200 N applied load; (**e**) Lithium disilicate with 100 N applied load; (**f**) Lithium disilicate with 200 N applied load.

It was observed that whenever the applied load increased by twofold, the calculated stress on the implant and bone also increased based on the values of the von Mises stresses, which were extracted using the finite element approach. Using zirconia and chromium cobalt as superstructure materials for a mandibular posterior three-unit implant-supported model, it can be observed that the result of the stress obtained on the implant and bone is similar due to the convergence of their elastic moduli of 200 and 218 Gpa, respectively. Although the implant and bone experience the greatest stress when making use of lithium disilicate superstructure material, this material has an elastic modulus of 95 Gpa, as presented in Tables 3 and 4.

Table 3. Von Mises stresses under 100 N loading at central fossa.

Material	Max. Equivalent von Mises Stress, MPa													
	Second Implant-Supported Premolar							Second Implant-Supported Molar						
	Apical	Cortical-Cancellous Bone Interface	Cortical Bone	Middle Third (Thread for Implant) (Distal Side)	Middle Third (Thread for Implant) (Mesial Side)	Neck (Distal Side)	Neck (Mesial Side)	Apical	Cortical-Cancellous Bone Interface	Cortical Bone	Middle Third (Thread for Implant) (Distal Side)	Middle Third (Thread for Implant) (Mesial Side)	Neck (Distal Side)	Neck (Mesial Side)
Zirconia	0.16	0.79	1.17	0.10	0.17	0.50	0.44	0.25	1.13	0.42	0.10	0.18	0.36	0.41
Chrome alloy cobalt	0.14	0.71	0.99	0.09	0.17	0.79	0.38	0.23	0.93	0.37	0.10	0.22	0.27	0.38
Lithium disilicate	0.30	1.01	2.13	0.18	0.20	0.75	0.84	0.44	1.74	2.04	0.15	0.56	0.33	0.70

Table 4. Von Mises stresses under 200 N loading at central fossa.

Material	Max. Equivalent von Mises Stress, MPa													
	Apical	Cortical-Cancellous Bone Interface	Cortical Bone	Middle Third (Thread for Implant) (Distal Side)	Middle Third (Thread for Implant) (Mesial Side)	Neck (Distal Side)	Neck (Mesial Side)	Apical	Cortical-Cancellous Bone Interface	Cortical Bone	Middle Third (Thread for Implant) (Distal Side)	Middle Third (Thread for Implant) (Mesial Side)	Neck (Distal Side)	Neck (Mesial Side)
Zirconia	0.32	1.96	2.34	0.20	0.21	1.92	0.73	0.47	1.65	0.73	0.18	0.22	0.44	0.83
Chrome alloy cobalt	0.34	1.68	2.31	0.21	0.15	0.84	0.87	0.48	2.15	0.86	0.21	0.37	0.53	0.77
Lithium disilicate	0.54	2.07	3.28	0.33	0.70	1.50	1.53	0.88	3.50	1.31	0.35	0.74	0.59	1.53

Tables 5–8 present the descriptive statistics concerning the statistical analysis (ANOVA) and homogeneity of variances.

Table 5. Statistical analysis of obtained stresses of mandibular posterior implant-supported prosthesis under 100 N applied load with different superstructures materials.

Fixed Implant Prosthesis under 100 N		Nodes	Mean	Std. Deviation	Std. Error	95% Confidence Interval for Mean	
						Lower Bound	Upper Bound
Second implant-supported premolar	Zirconia	7	1.5829	0.92141	0.34826	0.7307	2.4350
	Cobalt chromium alloy	7	1.4914	0.83665	0.31622	0.7177	2.2652
	Lithium dislicate	7	2.3886	1.40046	0.52932	1.0934	3.6838
Second implant-supported molar	Zirconia	7	1.8886	1.44050	0.54446	0.5563	3.2208
	Cobalt chromium alloy	7	1.9014	1.39244	0.52629	0.6136	3.1892
	Lithium dislicate	7	2.4086	1.70436	0.64419	0.8323	3.9848

Table 6. Test of Homogeneity of Variances.

Fixed Implant Prosthesis under 100 N		Levene Statistic	df_1	df_2	Sig.
Second implant-supported premolar	Based on Mean	1.282	2	18	0.302
Second implant-supported molar	Based on Mean	0.125	2	18	0.883

Table 7. Statistical analysis of obtained stresses of mandibular posterior implant-supported prosthesis under 200 N applied load with different superstructures materials.

Fixed Implant Prosthesis under 200 N		Nodes	Mean	Std. Deviation	Std. Error	95% Confidence Interval for Mean	
						Lower Bound	Upper Bound
Second implant-supported premolar	Zirconia	7	3.2071	1.89507	0.71627	1.4545	4.9598
	Cobalt chromium alloy	7	3.2057	1.97693	0.74721	1.3774	5.0341
	Lithium dislicate	7	4.7771	2.85435	1.07884	2.1373	7.4170
Second implant-supported molar	Zirconia	7	3.5771	2.97831	1.12570	0.8227	6.3316
	Cobalt chromium alloy	7	3.5214	1.92237	0.72659	1.7435	5.2993
	Lithium dislicate	7	5.0629	3.36040	1.27011	1.9550	8.1707

Table 8. Test of Homogeneity of Variances.

Fixed Implant Prosthesis under 200 N		Levene Statistic	df_1	df_2	Sig.
Second implant-supported premolar	Based on Mean	0.846	2	18	0.446
Second implant-supported molar	Based on Mean	1.024	2	18	0.379

The *p* values for the test of homogeneity of variances (Levene's statistic) of the obtained results for the second implant-supported premolar and second implant-supported molar were 0.302 and 0.883, respectively. Given that it is greater than 0.05, this value is regarded as non-significant.

For the second implant-supported molar and second implant-supported premolar, the *p* values for the test of homogeneity of variances (Levene's statistic) were 0.379 and 0.446, respectively. Since the value is higher than 0.05, it is considered to be non-significant.

Based on the statistical analysis, all the resulting data are within the normal distribution, located between the upper and lower values according to the ANOVA test.

4. Discussion

In this study, we investigated the impact on the von Mises stresses as determined by the finite element analysis of using various superstructure materials with voracious applied loads in a mandibular posterior three-unit implant-supported prosthesis. The ability of a material to return to its original shape when the force that caused the deformation has subsided is known as elasticity. This study has established and demonstrated that the stress

generated is higher when the load is applied to a material with a lower Young's modulus of elasticity. It is proven that the Young's modulus is the ratio between stress and strain.

In dentistry, three-dimensional finite element studies are frequently utilized to approximate the stress distribution that takes place in prosthetic components, peri-implant bone, and the implant system [47].

The stresses resulting from simulating axial and buccolingual loading of three different types of FPDs in the natural tooth, the implant, and the entire prosthesis were compared by Jain H. et al. by using three different types of materials. They reported that the type of prosthesis materials did not appear to have a significant effect on the pattern of stress distribution in any of the models [48]. Assunção W. G. et al. concluded that the use of stiffer and softer superstructures materials did not affect the stress distribution and stress values in the supporting tissue [49]. Employing stiff materials with greater elastic moduli could result in increased stresses being applied to the bone surrounding the implant. Therefore, using more flexible materials, like acrylic, may reduce stress, particularly on atrophic bones [50]. According to Gungor and Yilmaz [51], models containing zirconia showed higher stress levels (93.6 MPa) than those containing lithium disilicate (76.3 MPa).

The present study showed how the elastic modulus of the materials will affect the stress distribution. Materials with a high elastic modulus, such as zirconia, produce the best stress distribution, unlike materials with lower elasticity such as lithium disilicate, which produce higher stresses.

Based on this simulation, the lowest stress values for the zirconia and chromium cobalt materials under an effective load of 100 Newtons were found to be in the middle third region of the implant-supported prosthesis, according to the analysis of the von Mises stress values. On the other hand, when employing lithium disilicate as a superstructure material under a load of 100 and 200 N, the greatest stress values were 2.13 and 3.28 MPa, respectively, in the cortical bone.

It is evident from looking at Figure 8a that when lithium disilicate is utilized as the superstructure material, the stress at the apical area is 50% higher than when the other materials are employed. It can be observed from the stress values that there are not many changes in the stress levels at the cortical–cancellous bone interface area. The largest discrepancies in stress levels between various superstructure materials can be found in the cortical bone region. When utilizing lithium disilicate, the stress value was at its greatest. The scenario in the middle third (distal side) area is the same as it was in previous areas. It was found that when employing lithium disilicate as opposed to other materials, the stress value is about twice as high. Regarding the stresses of the neck and middle third (mesial side), there were not many variations in the stress values, even when employing different superstructure materials.

In general, we noticed that the stress values in the apical and cortical–cancellous bone interface areas in the implant-supported molar were relatively higher than the stress in the same areas in the implant-supported premolar. When lithium disilicate was utilized as a superstructure material, the cortical bone region in the second implant-supported molar showed the highest stress value, as can be seen in Figure 8b. In contrast, there were only minor variations in the stress values in other regions with distinct superstructure materials.

Based on Figure 9a, we can infer that stress doubles in proportion to a doubling of applied force. It was found that the cortical bone and cortical–cancellous bone interface areas had the highest stress values in the implant-supported premolar. It is worth noting that the highest stress value was recorded for these areas when using lithium disilicate as the superstructure material. When using zirconia, chromium cobalt, and lithium disilicate materials, it can be observed that the stress values gradually increase for these materials respectively, recording the highest value in the cortical bone region using lithium disilicate. In this study, the load does not apply in multiple directions and multiple points. Static analysis was used to analyze stress distribution in vertical loads. In the future, researchers could conduct research using dynamic analysis in both vertical and horizontal loads.

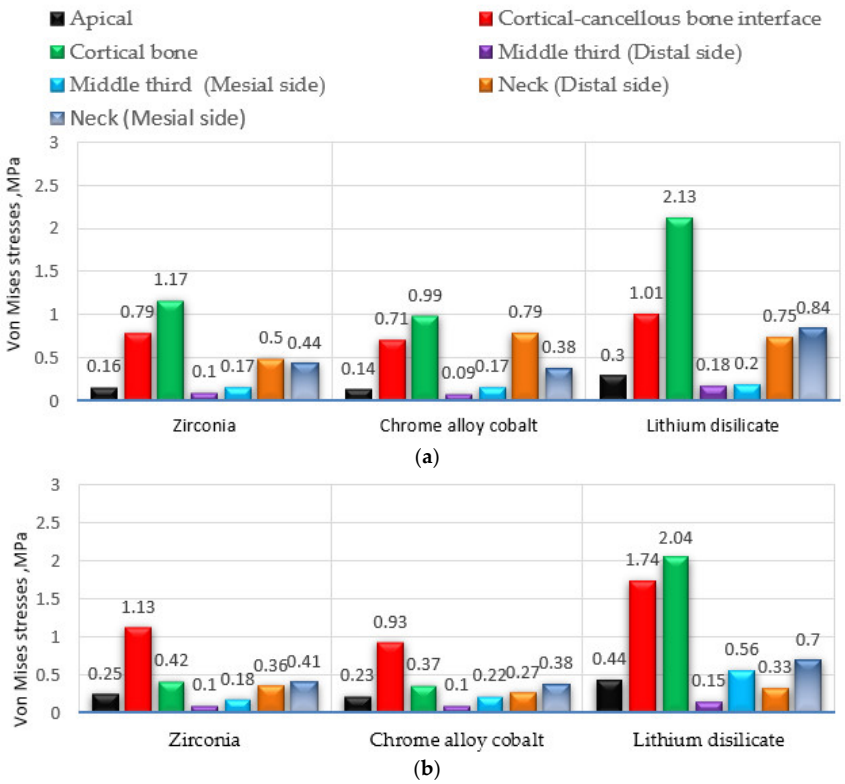


Figure 8. Graph showing von Mises stresses values by using different superstructure materials with 100 N applied load: (**a**) second implant-supported premolar; (**b**) Second implant-supported molar.

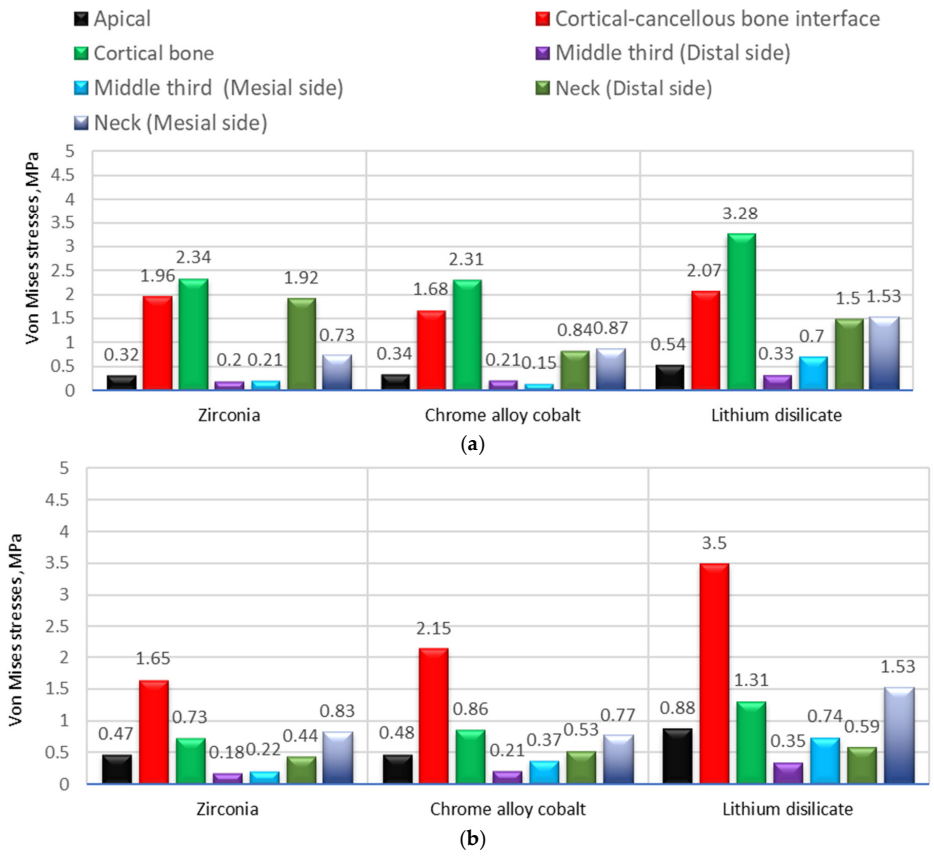


Figure 9. Graph showing von Mises stresses values by using different superstructure materials with 200 N applied load: (**a**) second implant-supported premolar; (**b**) Second implant-supported molar.

The null hypothesis indicates that stress distribution and stress values at the bone tissue surrounding an implant are unaffected by the use of more stiff or resilient material for the superstructure of an implant-supported prosthesis [34]. Dhanasekaran et al. [52] suggested that lithium disilicate resulted in lesser stresses among all the crown materials, similar to the findings [53] These were rejected since there was a difference in the stresses in the implant and bone as related to each simulated condition with different superstructure materials.

5. Conclusions

Based on the results and within the limitations of evaluating the stress distribution by 3D-FEA, it can be concluded that the difference in von Mises stress values in the bone and implant nodes areas is slight when using zirconia and cobalt chromium alloy as superstructure materials. When lithium disilicate is used, the areas in the implants and bones experience the highest stress values. Generally, for every doubling application of load, the stress on the implant-supported model doubles.

Zirconia and cobalt chromium alloy behave similarly in stress distribution because their mechanical characteristics, such as their elastic modulus, are similar. Based on the analysis of the data, zirconia and cobalt chromium alloy are suggested to be the best material to employ as the superstructure material when producing implant-supported prosthetics.

Author Contributions: R.M.J.: Conceptualization, Methodology, Software, Validation, Formal Analysis, Investigation, Resources, Data Curation, Writing—Original Draft Preparation. A.M.A.-K.: Supervision, Project Administration, Conceptualization, Methodology, Software, Validation, Formal Analysis, Investigation, Visualization, Supervision, Review & Editing. All authors have read and agreed to the published version of the manuscript.

Funding: This study received no external funding.

Institutional Review Board Statement: Not applicable.

Informed Consent Statement: Not applicable.

Data Availability Statement: The data are contained within the article. If any raw data supporting the conclusions are needed, the dataset can be made available upon request from the authors.

Acknowledgments: The authors are grateful to the Department of Prosthodontics, College of Dentistry, University of Baghdad, for providing them with the opportunity to complete this research.

Conflicts of Interest: The authors declare no conflicts of interest.

References

1. Santiago, J.F.; Verri, F.R.; Almeida, D.A.D.F.; De Souza Batista, V.E.; Lemos, C.A.A.; Pellizzer, E.P. Finite element analysis on influence of implant surface treatments, connection and bone types. *Mater. Sci. Eng. C* **2016**, *63*, 292–300. [CrossRef] [PubMed]
2. Alsmael, M.A.; Al-Khafaji, A.M. Evaluation of High-Performance Polyether Ether Ketone Polymer Treated with Piranha Solution and Epigallocatechin-3-Gallate Coating. *BioMed Res. Int.* **2024**, *2024*, 1741539. [CrossRef] [PubMed]
3. Hamad, T.I.; Fatalla, A.A.; Waheed, A.S.; Azzawi, Z.G.M.; Cao, Y.G.; Song, K. Biomechanical Evaluation of Nano-Zirconia Coatings on Ti-6Al-7Nb Implant Screws in Rabbit Tibias. *Curr. Med. Sci.* **2018**, *38*, 530–537. [CrossRef]
4. KN, C.; Eram, A.; Shetty, N.; Shetty, D.D.; Futane, M.; Keni, L.G. Evaluating Angled Abutments: Three-Dimensional Finite Element Stress Analysis of Anterior Maxillary Implants. *Prosthesis* **2024**, *6*, 315–328. [CrossRef]
5. Muhammed, S.A.; Al-Khafaji, A.M.; Al-Deen, H.H.J.J. The Influence of Strontium Oxide on the Physio-Mechanical Properties of Biomedical-Grade Titanium in Ti-SrO Composites. *J. Compos. Sci.* **2023**, *7*, 449. [CrossRef]
6. Tiwari, R.V.; Shakeel, S.K.; Gulia, S.K.; Biradar, J.M.; Agrawal, P.; Pandey, P.R. Straumann dental implant: A complete review. *Eur. J. Mol. Clin. Med.* **2022**, *9*, 579–587.
7. Fiorillo, L.; Milone, D.; D'Andrea, D.; Santonocito, D.; Risitano, G.; Cervino, G.; Cicciù, M. Finite Element Analysis of Zirconia Dental Implant. *Prosthesis* **2022**, *4*, 490–499. [CrossRef]
8. Zarone, F.; Di Mauro, M.I.; Ausiello, P.; Ruggiero, G.; Sorrentino, R. Current status on lithium disilicate and zirconia: A narrative review. *BMC Oral Health* **2019**, *19*, 134. [CrossRef]
9. Surgery, M.; Ibraheem, N.S.; Al-Adili, S.S. Assessment of dental Assessment of dental implant stability during healing period and determination of the factors that affect implant stability by means of resonance frequency analysis (Clinical study). *J. Bagh. Coll. Dent.* **2015**, *27*. Available online: https://jbcd.uobaghdad.edu.iq/index.php/jbcd/article/view/815 (accessed on 31 July 2024).

10. Ercal, P.; Taysi, A.E.; Ayvalioglu, D.C.; Eren, M.M.; Sismanoglu, S. Impact of peri-implant bone resorption, prosthetic materials, and crown to implant ratio on the stress distribution of short implants: A finite element analysis. *Med. Biol. Eng. Comput.* **2021**, *59*, 813–824. [CrossRef]
11. Rudolf, R.; Majerič, P.; Lazić, V.; Raić, K.T. Processing of Cobalt-Chrome Dental Alloys. In *Advanced Dental Metallic Materials*; Springer: Cham, Switzerland, 2024.
12. Barua, S.L.; Poduval, T.S.; Rani, S.; Jain, N.; Thakur, S. Stress distribution in bone around an implant-supported three-unit fixed dental prosthesis using two different computer-aided designing/computer-aided milling provisional crown materials: Milled polymethylmethacrylate and milled polyetheretherketone—A finite element analysis. *Dent. Res. J.* **2023**, *20*, 33.
13. Piconi, C.; Sprio, S. Oxide bioceramic composites in orthopedics and dentistry. *J. Compos. Sci.* **2021**, *5*, 206. [CrossRef]
14. Abdelraouf, R.M.; Tsujimoto, A.; Hamdy, T.M.; Alhotan, A.; Jurado, C.A.; Abadir, M.; Habib, N.A. The Effect of Surface Treatments of Presintered Zirconia on Sintered Surfaces. *J. Compos. Sci.* **2023**, *7*, 396. [CrossRef]
15. Magnani, G.; Fabbri, P.; Leoni, E.; Salernitano, E.; Mazzanti, F. New perspectives on zirconia composites as biomaterials. *J. Compos. Sci.* **2021**, *5*, 244. [CrossRef]
16. Vieira, F.R.; Bitencourt, S.B.; Rosa, C.D.D.R.D.; Vieira, A.B.; dos Santos, D.M.; Goiato, M.C. Influence of Different Restoring Materials on Stress Distribution in Prosthesis on Implants: A Review of Finite Element Studies. *Eur. J. Dent.* **2023**, *17*, 001–006. [CrossRef]
17. de Souza Batista, V.E.; Verri, F.R.; de Faria Almeida, D.A.; Santiago Junior, J.F.; Lemos, C.A.A.; Pellizzer, E.P. Evaluation of the effect of an offset implant configuration in the posterior maxilla with external hexagon implant platform: A 3-dimensional finite element analysis. *J. Prosthet. Dent.* **2017**, *118*, 363–371. [CrossRef]
18. Geringer, A.; Diebels, S.; Nothdurft, F.P. Influence of superstructure geometry on the mechanical behavior of zirconia implant abutments: A finite element analysis. *Biomed. Tech.* **2014**, *59*, 501–506. [CrossRef]
19. Ferreira, M.B.; Barão, V.A.; Faverani, L.P.; Hipólito, A.C.; Assunção, W.G. The role of superstructure material on the stress distribution in mandibular full-arch implant-supported fixed dentures. A CT-based 3D-FEA. *Mater. Sci. Eng. C* **2014**, *35*, 92–99. [CrossRef] [PubMed]
20. Bidra, A.; Rungruanganunt, P.; Gauthier, M. Clinical outcomes of full arch fixed implantsupported zirconia prostheses: A systematic review. *Eur. J. Oral Implantol.* **2017**, *10*, 35–45.
21. D'amico, C.; Bocchieri, S.; Sambataro, S.; Surace, G.; Stumpo, C.; Fiorillo, L. Occlusal Load Considerations in Implant-Supported Fixed Restorations. *Prosthesis* **2020**, *2*, 252–265. [CrossRef]
22. Shakir, S.M.; Muhsin, S.A.; Al Marza, R.S. FEM: Mono-implant cement-retained crown with two-different adhesive materials. *J. Baghdad Coll. Dent.* **2023**, *35*, 37–48. [CrossRef]
23. Ahmed, S.A.S.; Eldosoky, M.A.A.; El-Wakad, M.T. Effect of Stiffness of Single Implant Supported Crowns on the Resultant Stresses: A Finite Element Analysis. *Egypt. J. Hosp. Med.* **2016**, *63*, 172–184. [CrossRef]
24. Gökçimen, G.; Durkan, R.; Deste Gökay, G.; Oyar, P. The effect of different abutment and restorative crown materials on stress distribution in single-unit implant-supported restorations: A 3D finite element stress analysis. *J. Prosthodont.* **2023**, *33*, 497–505. [CrossRef]
25. Al Jabbari, Y.S. Physico-mechanical properties and prosthodontic applications of Co-Cr dental alloys: A review of the literature. *J. Adv. Prosthodont.* **2014**, *6*, 138–145. [CrossRef]
26. Edelhoff, D.; Güth, J.F.; Erdelt, K.; Brix, O.; Liebermann, A. Clinical performance of occlusal onlays made of lithium disilicate ceramic in patients with severe tooth wear up to 11 years. *Dent. Mater.* **2019**, *35*, 1319–1330. [CrossRef]
27. Furtado de Mendonca, A.; Shahmoradi, M.; de Gouvêa, C.V.D.; De Souza, G.M.; Ellakwa, A. Microstructural and Mechanical Characterization of CAD/CAM Materials for Monolithic Dental Restorations. *J. Prosthodont.* **2018**, *28*, E587–E594. [CrossRef]
28. Forster, A.; Ungvári, K.; Györgyey, Á.; Kukovecz, Á.; Turzó, K.; Nagy, K. Human epithelial tissue culture study on restorative materials. *J. Dent.* **2014**, *42*, 7–14. [CrossRef] [PubMed]
29. Ariaans, K.; Heussen, N.; Schiffer, H.; Wienert, A.; Plümäkers, B.; Rink, L.; Wolfart, S. Use of molecular indicators of inflammation to assess the biocompatibility of all-ceramic restorations. *J. Clin. Periodontol.* **2016**, *43*, 173–179. [CrossRef]
30. Baldissara, P.; Llukacej, A.; Ciocca, L.; Valandro, F.L.; Scotti, R. Translucency of zirconia copings made with different CAD/CAM systems. *J. Prosthet. Dent.* **2010**, *104*, 6–12. [CrossRef]
31. Chen, Y.W.; Moussi, J.; Drury, J.L.; Wataha, J.C. Zirconia in biomedical applications. *Expert Rev. Med. Devices* **2016**, *13*, 945–963. [CrossRef]
32. Bacchi, A.; Boccardi, S.; Alessandretti, R.; Pereira, G.K.R. Substrate masking ability of bilayer and monolithic ceramics used for complete crowns and the effect of association with an opaque resin-based luting agent. *J. Prosthodont. Res.* **2019**, *63*, 321–326. [CrossRef] [PubMed]
33. Kim, S.Y.; Kim, B.S.; Kim, H.; Cho, S.Y. Occlusal stress distribution and remaining crack propagation of a cracked tooth treated with different materials and designs: 3D finite element analysis. *Dent. Mater.* **2021**, *37*, 731–740. [CrossRef] [PubMed]
34. Sevimay, M.; Usumez, A.; Eskitascioglu, G. The influence of various occlusal materials on stresses transferred to implant-supported prostheses and supporting bone: A three-dimensional finite-element study. *J. Biomed. Mater. Res. Part B Appl. Biomater.* **2005**, *73B*, 140–147. [CrossRef] [PubMed]
35. Santonocito, D.; Nicita, F.; Risitano, G. A Parametric Study on a Dental Implant Geometry Influence on Bone Remodelling through a Numerical Algorithm. *Prosthesis* **2021**, *3*, 157–172. [CrossRef]

36. Boukhlif, A.; Merdji, A.; Roy, S.; Alkhaldi, H.; Abu-Alshaikh, I.; Della, N.; Cristache, C.M.; Hillstrom, R. Effect of supporting implants inclination on stability of fixed partial denture: A finite element study. *Proc. Inst. Mech. Eng. Part H J. Eng. Med.* **2020**, *234*, 1162–1171. [CrossRef]
37. Jassim, R.K. *Finite Element Stress Analysis and Radiographic Follow-up of Mandibular Implant Retained—Overdenture [Original]*; University of Baghdad: Baghdad, Iraq, 2006.
38. Jassim, R.K.; Ibrahim, I.K. Finite Element Stress Analysis Study for Stresses around Mandibular Implant Retained Overdenture MIR-OD. *J. Baghdad Coll. Dent.* **2014**, *26*, 30–36. [CrossRef]
39. Phulari, R.G.S. *Textbook of Dental Anatomy, Physiology and Occlusion*; JP Medical Ltd.: London, UK, 2013.
40. Guedes, C.A.S.; Matos, R.A.; da Gama Ramos, G.; de Souza Júnior, A.R. Finite element analysis of the stress generated by the type of restorative material in the implant crown system. *Braz. J. Health Rev.* **2024**, *7*, 324–347. [CrossRef]
41. Kilic, E.; Doganay, O. Evaluation of stress in tilted implant concept with variable diameters in the atrophic mandible: Three-dimensional finite element analysis. *J. Oral Implant.* **2020**, *46*, 19–26. [CrossRef]
42. Al-naqshabandi, F.I.; Selivany, B.J.; Al-zahawi, A.R. Biomechanical Behavior of Lithium-Disilicate-Modified Endocrown Restorations: A Three-Dimensional Finite Element Analysis. *Ceramics* **2023**, *6*, 2162–2177. [CrossRef]
43. Faisal, E.; Hamza, T.; Mokhtar, A. Finite Element Analysis of Monolithic PEEK and Zirconia Fixed Dental Prosthesis (In Vitro Study). *J. Fundam. Clin. Res.* **2023**, *3*, 1–15. [CrossRef]
44. Sannino, G.; Pozzi, A.; Schiavetti, R.; Barlattani, A. Stress distribution on a three-unit implant-supported zirconia framework. A 3d finite element analysis and fatigue test. *Oral Implantol.* **2012**, *5*, 11.
45. Byun, S.-H.; Seo, J.-H.; Cho, R.-Y.; Yi, S.-M.; Kim, L.-K.; Han, H.-S.; On, S.-W.; Kim, W.-H.; An, H.-W.; Yang, B.-E. Finite Element Analysis of a New Non-Engaging Abutment System for Three-Unit Implant-Supported Fixed Dental Prostheses. *Bioengineering* **2022**, *9*, 483. [CrossRef] [PubMed]
46. Al-Judy, H.J. *Selection of Mandibular Distal Extension Fixed Implant Supported Prosthesis Design Using 3-D Finite Element [Original]*; University of Baghdad: Baghdad, Iraq, 2005.
47. Fatalla, A.A.; Song, K.; Du, T.; Cao, Y. A Three-Dimensional Finite Element Analysis for Overdenture Attachments Supported by Teeth and/or Mini Dental Implants. *J. Prosthodont.* **2012**, *21*, 604–613. [CrossRef]
48. Jain, H.; Kalra, T.; Kumar, M.; Bansal, A.; Jain, D. Three-Dimensional Finite Element Analysis to Evaluate Stress Distribution in Tooth and Implant-Supported Fixed Partial Denture–An In Vitro Study. *Dent. J. Adv. Stud.* **2020**, *8*, 084–091. [CrossRef]
49. Assunção, W.G.; Gomes, É.A.; Barão, V.A.R.; Delben, J.A.; Tabata, L.F.; De Sousa, E.A.C. Effect of superstructure materials and misfit on stress distribution in a single implant-supported prosthesis: A finite element analysis. *J. Craniofacial Surg.* **2010**, *21*, 689–695. [CrossRef]
50. Haroun, F.; Ozan, O. Evaluation of stresses on implant, bone, and restorative materials caused by different opposing arch materials in hybrid prosthetic restorations using the all-on-4 technique. *Materials* **2021**, *14*, 4308. [CrossRef]
51. Bankoğlu Güngör, M.; Yılmaz, H. Evaluation of stress distributions occurring on zirconia and titanium implant-supported prostheses: A three-dimensional finite element analysis. *J. Prosthet. Dent.* **2016**, *116*, 346–355. [CrossRef]
52. Dhanasekaran, T.; Andonissamy, L.; Abdullah, F.; Paramasivam, Y.S. Effect of different occlusal materials on peri-implant stress distribution with different osseointegration condition: A finite element analysis. *J. Indian Prosthodont. Soc.* **2024**, *24*, 292–299.
53. Makhija, S.K.; Lawson, N.C.; Gilbert, G.H.; Litaker, M.S.; McClelland, J.A.; Louis, D.R.; Gordan, V.V.; Pihlstrom, D.J.; Meyerowitz, C.; Mungia, R.; et al. Dentist material selection for single-unit crowns: Findings from the National Dental Practice-Based Research Network. *J. Dent.* **2016**, *55*, 40–47. [CrossRef]

Disclaimer/Publisher's Note: The statements, opinions and data contained in all publications are solely those of the individual author(s) and contributor(s) and not of MDPI and/or the editor(s). MDPI and/or the editor(s) disclaim responsibility for any injury to people or property resulting from any ideas, methods, instructions or products referred to in the content.